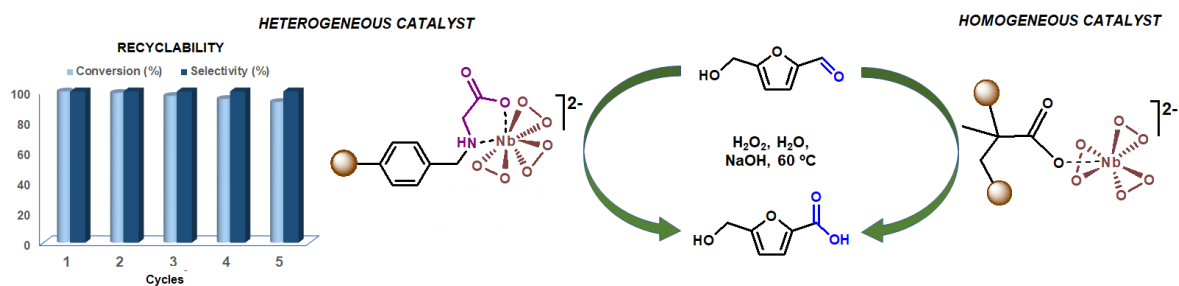


## CHAPTER 4

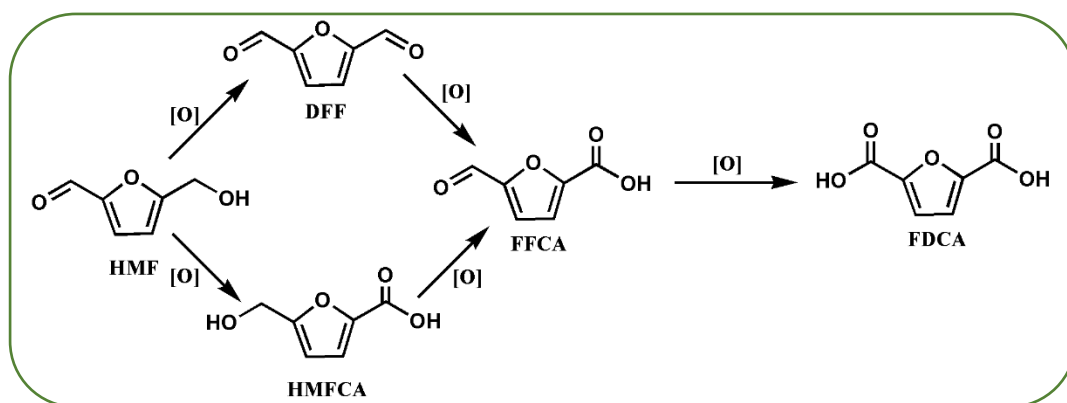
### Selective and Mild Oxidation of 5-Hydroxymethylfurfural to 5-Hydroxymethyl-2-Furancarboxylic Acid over Organic Polymer-Supported Peroxido-niobium(V) Catalysts



## 4.1 Introduction

Over the past decade, enormous efforts have been dedicated to exploiting the abundant and renewable biomass resources for the production of sustainable biofuels and generating bulk and fine chemicals to overcome the growing scarcity of non-renewable fossil resources such as oil and natural gas [1-3]. The application of niobium-based solid catalysts in conversion of biomass for the production of various platform chemicals and biofuel, have been attracting considerable contemporary interest [4-7], although such systems have rarely been investigated in 5-hydroxymethyl-2-furfural (HMF) oxidations to obtain different value-added products [4-6].

5-Hydroxymethyl-2-furfural, the key platform molecule acting as a link between biomass and chemicals, has been considered as the most suitable bio-derived building block to reduce the dependence on non-renewable petrochemical resources, owing to its ready availability from biorefinery carbohydrates [8-10]. Myriads of reports are available pertaining to the oxidation of HMF to a large variety of value-added compounds such as 5-hydroxymethyl-2-furancarboxylic acid (HMFCFA), 2,5-diformylfuran (DFF), 5-formyl-2-furancarboxylic acid (FFCA), levulinic acid (LA) and 2,5-furandicarboxylic acid (FDCA) (**Scheme 4.1**) by using various biological [11-13] and chemical catalysts [14-16]. All of these HMF derivatives are valuable precursors for bioplastics [17-19], functional polymers [15,16,20], pharmaceuticals [15,16,21], biofuel additives, etc. [7,15,16,22,23]. Recently, Kucherov and the group comprehensively reviewed the advancements in the field of biomass-derived C<sub>6</sub>-furanic platform chemicals, mainly by focusing on the significant chemical reactions for sustainable processing of the biomass [22].



**Scheme 4.1** Schematic representation of biomass conversion into value-added chemicals.

---

5-Hydroxymethyl-2-furancarboxylic acid (HMFCFA) is a relatively lesser explored product formed by the selective oxidation of the aldehydic group of HMF (**Scheme 4.1**) [11,22,24]. The partially oxidized HMFCFA, in addition to being an intermediate in FDCA synthesis and a useful monomer for a variety of polyesters [20], is also known to exhibit antitumor and antimicrobial activities [11,21]. However, in contrast to substantial research on the synthesis of FDCA and DFF from HMF [9,15,16,22,23], there are much fewer reports dealing with the targeted synthesis of HMFCFA [24-27]. This is likely to be due to the difficulty encountered in the selective oxidation of the formyl group of HMF into carboxylic acid without affecting its alcohol functional group [27]. Nevertheless, apart from the classic Cannizzaro reaction [28,29], a number of promising catalytic methodologies have been developed lately for the oxidation of HMF to HMFCFA [24-27,30-33]. Aerobic oxidation of HMF to HMFCFA with 87% selectivity was reported by Zhang *et al.* using a montmorillonite K-10 clay supported molybdenum catalyst in toluene [27]. The majority of the available catalytic procedures for HMFCFA synthesis are based on aerobic oxidation of HMF over noble metals like Au, Ag, Pd, etc. [24-26,30-32], which generally utilize air or molecular oxygen at high oxygen pressure. For example, an O<sub>2</sub> pressure of 690 kPa was used to obtain high yields (90-95%) of HMFCFA over supported gold catalysts such as acidic carbons supported Au nanoparticles [30], Au/C, and Au/TiO<sub>2</sub> catalysts [31]. Schade *et al.* achieved 98% HMFCFA selectivity using Ag/ZrO<sub>2</sub> catalyst under high oxygen pressure (50 °C, 10 bar O<sub>2</sub>, 4 equivalents of aqueous NaOH) [25]. In another recent work, Ag-polyvinylpyrrolidone (PVP) supported on ZrO<sub>2</sub>, provided 100% HMF conversion with 98% yield of HMFCFA in aerobic oxidation of HMF [26].

We have so far come across only two reports on liquid-liquid phase oxidation of HMF to obtain HMFCFA using H<sub>2</sub>O<sub>2</sub> as oxidant [34,35], although hydrogen peroxide has been successfully used as the liquid oxygen source in biomass conversion [36,37]. Zhao *et al.* recently reported impressive HMFCFA yield of 98% achieved with Ag<sub>2</sub>O based catalyst using H<sub>2</sub>O<sub>2</sub> as oxidant in aqueous Na<sub>2</sub>CO<sub>3</sub> solution (1h, 90 °C) [34]. A heterogeneous catalyst of Ag<sub>2</sub>O supported on CaCO<sub>3</sub> developed by T. Su and group also afforded selective oxidation of HMF (89% conversion) to HMFCFA (95% selectivity) with H<sub>2</sub>O<sub>2</sub> in both conventional heating (100 °C) and microwave-assisted batch conditions (conversion/selectivity: 95%/97%) [35]. In both the aforementioned cases however, catalysts deactivation was reported during recyclability experiments due to

---

partial reduction of Ag(I) to metallic silver [34,35]. In fact, apart from difficulty in catalyst regeneration factors such as long reaction time, high cost of the catalyst, requirement of high O<sub>2</sub> pressure and high temperature remain key issues associated with many of the otherwise promising noble-metal based HMF oxidation procedures [24,25,30-33]. Moreover, to our knowledge, none of the existing high yielding procedures reported 100% HMFCFA selectivity. Thus, from the economic and ecological perspectives, development of innovative, stable and recyclable, non-noble metal-based catalysts for selective conversion of HMF to HMFCFA is still highly desired [4,38].

Activity of Nb-based zeolites and mesoporous Nb-MCM-41 materials as catalysts in synthesis of FDCA [5] and DFF [6], respectively have been investigated recently. Interestingly, we have so far come across only one report mentioning the conversion of HMF (>85%) to selective formation of HMFCFA (>90%) achieved by using Nb-based nanocomposites during the targeted synthesis of FDCA [4]. The reaction however employed organic peroxide, *tert*-butyl hydroperoxide (TBHP) as oxidant and required a high reaction temperature (100 °C), and 12 h of reaction time, which compromised the overall environmental compatibility of the procedure [4].

An inspection of relevant literature showed that the application of polymers as supports for the grafting of active peroxidometal systems in catalyst design for HMF oxidation remains yet to be explored [26,39,40]. Our findings presented in Chapter 3 amply demonstrated the high efficiency of PS-DVB resin supported pNb catalysts in epoxidation of variety olefins as well as chemoselective oxidation of sulfides with H<sub>2</sub>O<sub>2</sub>.

As a direct sequel to our work presented in Chapter 3, in the present work, we considered it worthwhile to examine the activity of the **MR** supported solid peroxidoniobium (pNb) complexes, [Nb(O<sub>2</sub>)<sub>3</sub>(val)]<sup>2-</sup>-**MR** (**3.1**) [Nb(O<sub>2</sub>)<sub>3</sub>(asn)]<sup>2-</sup>-**MR** (**3.2**) and [Nb(O<sub>2</sub>)<sub>3</sub>(gly)]<sup>2-</sup>-**MR** (**3.3**) as potential catalysts for HMFCFA synthesis *via* HMF oxidation using H<sub>2</sub>O<sub>2</sub> as oxidant. Moreover, we have decided to develop a homogeneous catalyst system by anchoring pNb species to a linear WSP and to carry out a comparative investigation on catalytic efficiency of the two distinct categories of compounds in HMF oxidation with H<sub>2</sub>O<sub>2</sub> in aqueous medium. Apart from the prospect of creating possible water-tolerant oxidation catalysts usable in aqueous media, our additional interest in obtaining water-soluble macromolecular pNb systems with bio-relevant attributes, provided the impetus to direct our efforts to synthesize pNb complex stabilized in a soluble macro-ligand environment.

---

Herein we present the synthesis and characterization of a new macromolecular pNb complex immobilized on WSP, poly(sodium methacrylate) (**PMA**). The activity of **MR** supported catalysts **3.1-3.3** as well as the soluble complex  $[\text{Nb}(\text{O}_2)_3(\text{carboxylate})]^{2-}$ -**PMA** (**NbPMA**, **4.1**) as heterogeneous or homogeneous catalysts in selective oxidation of HMF with  $\text{H}_2\text{O}_2$  as the oxidant in an aqueous medium has been investigated. The reaction conditions were optimized for the targeted synthesis of HMFCA and activities of both types of catalysts were compared. The efficacy of the established catalytic methodology in terms of HMF conversion, HMFCA selectivity, turnover number (TON), recyclability as well as sustainability has been fully discussed. To our knowledge, this is the first report demonstrating the activity of polymer-supported peroxidoniobium (pNb) compounds as catalysts in HMF oxidation.

## 4.2 Experimental section

### 4.2.1 Synthesis of $[\text{Nb}(\text{O}_2)_3(\text{carboxylate})]^{2-}$ -PMA (**NbPMA**) (**4.1**)

The precursor complex  $\text{Na}_3[\text{Nb}(\text{O}_2)_4] \cdot 13\text{H}_2\text{O}$  (**TpNb**) was prepared by following the reported method [41] which has already been described in the Chapter 3. To a solution of the precursor complex (0.65 g, 1.25 mmol) in 30%  $\text{H}_2\text{O}_2$  (4 mL), the aqueous poly(sodium-methacrylate) solution (1 mL) was dropwise added with constant stirring, maintaining an ice bath condition ( $<4^\circ\text{C}$ ). After continuously stirring for about 1 h in an ice bath a clear solution of  $\text{pH} \approx 7$  was obtained. The solution was kept at  $<4^\circ\text{C}$  for 3 h of contact time and then treated with pre-cooled acetone to induce precipitation. After decanting the supernatant liquid, the white pasty residue was repeatedly treated with acetone under scratching. The microcrystalline product could be separated by centrifugation and dried *in vacuo* over concentrated sulfuric acid.

### 4.2.2 Procedure for the oxidation of HMF to HMFCA

In a typical reaction, HMF (0.4 mmol, 50.4 mg) was dissolved in water (4 mL) in a 50 mL round-bottomed flask. Subsequently, aqueous NaOH solution (32 mg, 0.8 mmol) and the niobium catalyst (29.6 mg, 0.008 mmol of Nb) was added to it under continuous stirring. This was followed by the dropwise addition of aqueous 30%  $\text{H}_2\text{O}_2$  (0.09 mL, 0.8 mmol) to the reaction mixture maintaining a flow rate of  $9 \mu\text{L}/\text{min}$  with constant stirring. The reaction was conducted at  $60^\circ\text{C}$  maintaining the molar ratio of HMF: oxidant at 1:2 and Nb: HMF molar ratio at 1:50. After completion of the reaction,

---

the catalyst was separated from the reaction mixture, and the products were analyzed by HPLC (**Appendix III**).

A high-performance liquid chromatography system (Thermo Scientific Dionex Ultimate 3000 HPLC) equipped with a UV detector and a reversed-phase C18 column (250 × 4.6 mm) was used for quantitative analysis of HMF and HMFCa. The maximum detection wavelength was 280 nm and the column temperature were maintained at 25 °C. The mobile phase comprised of methanol, 0.1 wt.% of the aqueous acetic acid solution, acetonitrile, and water, and their composition and flow rate varied with time due to the applied gradient method. The products were identified by comparing the retention time with the corresponding commercial standard compounds. The external standard method was employed to calculate the conversion of HMF and the HMFCa yield.

Conversion of HMF and yield of HMFCa were calculated using the following equations:

$$\text{HMF conversion (\%)} = \frac{\text{mmol of HMF converted after the reaction}}{\text{Initial mmol of HMF}} \times 100\% \quad (4.1)$$

$$\text{HMFCa yield (\%)} = \frac{\text{mmol of HMFCa formed after the reaction}}{\text{Initial mmol of HMF}} \times 100\% \quad (4.2)$$

#### 4.2.3 Procedure for control experiment

The control or blank reaction was conducted in absence of the catalyst at 60 °C. The reaction proceeded as follows: to an aqueous solution of HMF (0.4 mmol HMF in 4 mL water) aqueous NaOH solution (32 mg, 0.8 mmol) was added which was followed by the dropwise addition of aqueous 30% H<sub>2</sub>O<sub>2</sub> (0.09 mL, 0.8 mmol) with constant stirring.

#### 4.2.4 Catalyst regeneration

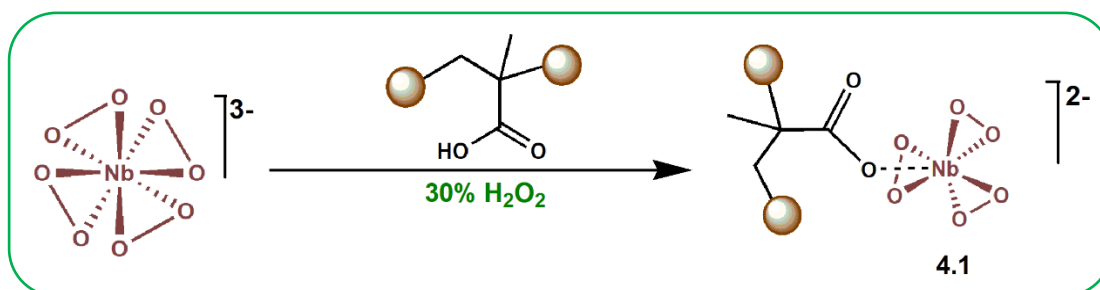
The catalyst **MRGNb (3.3)** could easily be recycled for five consecutive cycles. After running the first reaction cycle up to the stipulated time (90 min), the catalyst was separated from the reaction mixture by simple filtration or centrifugation, then washed with acetone and vacuum dried. The recovered catalyst was applied in a fresh reaction batch of the substrate with the addition of an aqueous NaOH solution and 30% H<sub>2</sub>O<sub>2</sub>,


maintaining the optimized reaction conditions. The content of the reaction mixture (reactant and products) was analyzed by HPLC.

### 4.3 Result and discussion

#### 4.3.1 Synthesis

The synthetic strategies adopted for preparing the water-soluble complex **NbPMA (4.1)** is summarized in **Scheme 4.2**. Utilizing the inherent propensity of water-soluble polymers (WSP) with pendant ligand groups to bind metal ions, workers from our laboratory have earlier devised rather straightforward and facile strategies to incorporate peroxidometal complexes into soluble macromolecular supports [42-46]. In the present study, the water-soluble compound, **NbPMA (4.1)** was synthesized by reacting the tetraperoxidoniobium complex  $\text{Na}_3[\text{Nb}(\text{O}_2)_4]$  (TpNb) with carboxylate containing WSP, poly(sodium-methacrylate) in presence of hydrogen peroxide, in aqueous medium at neutral pH (**Scheme 4.2**). The compound was isolated by inducing precipitation with acetone. It is notable that, for the successful formation of the catalyst maintenance of a temperature of  $<4\text{ }^\circ\text{C}$ , a stipulated contact time and a near-neutral pH of the reaction medium was observed to be critical parameters.



**Scheme 4.2** Synthesis of WSP-supported pNb catalyst. “” represents polymer chain.

#### 4.3.2 Characterization

The niobium loading in the complex **NbPMA (4.1)** on the basis of Nb content obtained from ICP-OES and EDX analysis was found to be 1.33 mmol/g of the polymer. The elemental analysis data presented in **Table 4.1** showed the ratio of Nb: peroxide in the complex to be 1:3 indicating the occurrence of three peroxido groups around the Nb(V) center. The occurrence of Nb in the compound in its +5 oxidation state was evident from the diamagnetic nature of the complex as revealed by the magnetic susceptibility measurement.

**Table 4.1:** Analytical data for the synthesized complex **NbPMA (4.1)**

Complex	% Found from elemental analysis (% obtained from EDX spectra)				O <sub>2</sub> <sup>2-</sup>	Nb: O <sub>2</sub> <sup>2-</sup>	Nb loading <sup>a</sup> (mmol g <sup>-1</sup> of polymer)
	C	H	Na	Nb			
<b>NbPMA</b>	24.21 (24.51)	4.83 -	- (16.82)	12.63 <sup>b</sup> (12.39)	12.60 -	1:3	1.33 -

$$^a\text{Metal loading} = \frac{\text{Observed metal\%} \times 10}{\text{Atomic weight of metal}}$$

<sup>b</sup>Determined by ICP-OES analysis

#### 4.3.2.1 SEM and EDX analysis

Scanning electron microscopy was performed to assess the surface morphology and chemical composition in the complex as well as the respective neat polymer support. The micrographs (**Fig. 4.1**) showed considerable changes on the surface of the Nb loaded polymeric compounds in comparison to the relatively even surface of the pristine polymer. The clearly visible randomly oriented depositions of Nb species on the external surface of the compounds suggested that the anchored metal complexes are distributed across the polymeric surface of the complex.

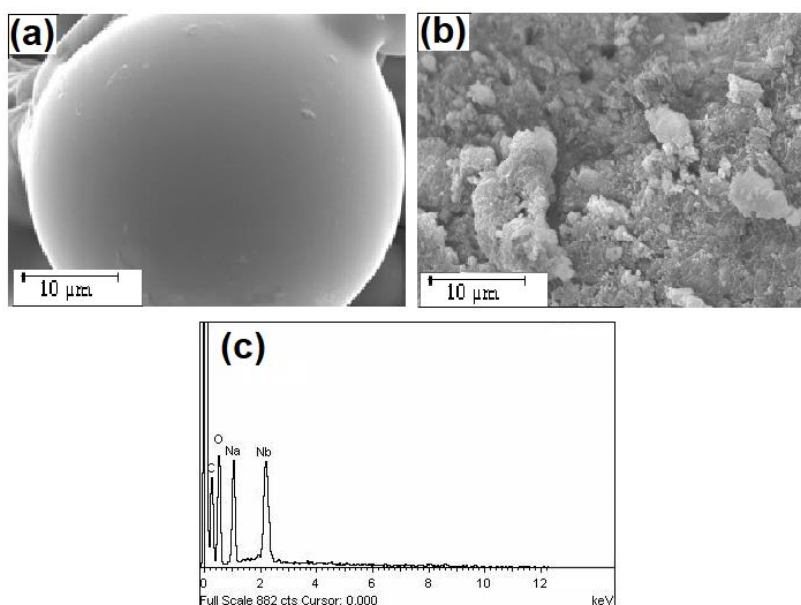


**Fig. 4.1** SEM images of (a) **PMA**, (b) **NbPMA** and (c) EDX spectrum of **NbPMA**.

Energy Dispersive X-ray analysis results showed the presence of Nb along with C, H, N, and Na as constituents of the complex. The EDX analysis [**Fig. 4.1** (c)] was carried out by focusing multiple regions on the surface of the complex. The composition



of the compound as obtained from EDX analysis agreed well with the elemental analysis data.

#### 4.3.2.2 FTIR and Raman spectral analysis

The FTIR spectra of the polymer-supported compound **NbPMA (4.1)** and the respective host polymer are illustrated in **Fig. 4.2**. The complementary Raman spectra of the compound is shown in **Fig. 4.3**. The empirical peak assignments were made based on the available literature. The FTIR and Raman spectra of the compound **4.1** provided evidence for the presence of  $[\text{Nb}(\text{O}_2)_3]^-$  moiety in the compounds by showing three well-resolved absorptions attributable to the  $\nu(\text{O-O})$  modes of  $\eta^2$ -peroxido group in the expected range of  $800\text{-}900\text{ cm}^{-1}$  along with  $\nu_{\text{asym}}(\text{Nb-O}_2)$  and  $\nu_{\text{sym}}(\text{Nb-O}_2)$  bands in the  $500\text{-}600\text{ cm}^{-1}$  region [47-49]. A triperoxidoniobium species, according to the established empirical rule, generally exhibits three  $\nu(\text{O-O})$  modes in the IR spectrum [47,49]. In addition, the spectrum of the poly(methacrylate) bound complex showed the peaks due to  $\nu_{\text{asym}}(\text{COO})$  and  $\nu_{\text{sym}}(\text{COO})$  of the carboxylate group at a relatively higher frequency of  $1655\text{ cm}^{-1}$  and lower frequency of  $1407\text{ cm}^{-1}$ , respectively (**Fig. 4.2**) compared to those observed for the pure poly(methacrylate) (**PMA**) at *ca.*  $1543\text{ [}\nu_{\text{asym}}(\text{COO})\text{]}$  and  $1415\text{ cm}^{-1}\text{ [}\nu_{\text{sym}}(\text{COO})\text{]}$ , respectively [44,50]. The distinct shift of  $\nu_{\text{asym}}(\text{COO})$  and  $\nu_{\text{sym}}(\text{COO})$  bands upon incorporation of pNb moiety onto the polymer **PMA**, resulting in significant increase in difference between  $\nu_{\text{asym}}(\text{COO})$  and  $\nu_{\text{sym}}(\text{COO})$  frequencies ( $\Delta\nu = 248\text{ cm}^{-1}$ )

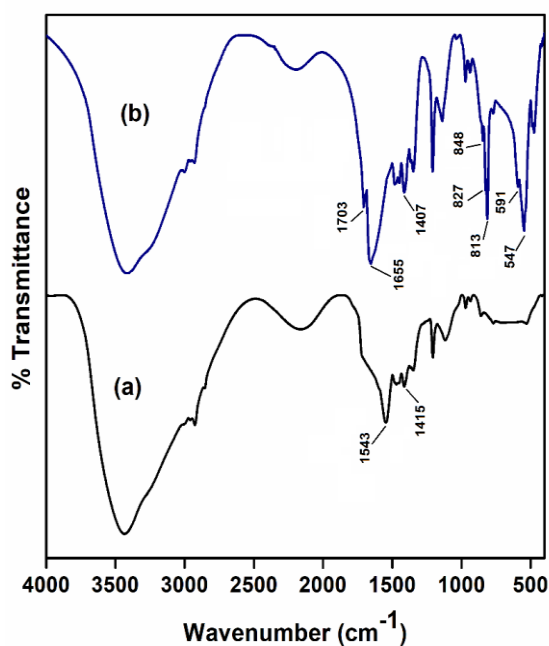


**Fig. 4.2** FTIR spectra of (a) **PMA** and (b) **NbPMA (4.1)**.

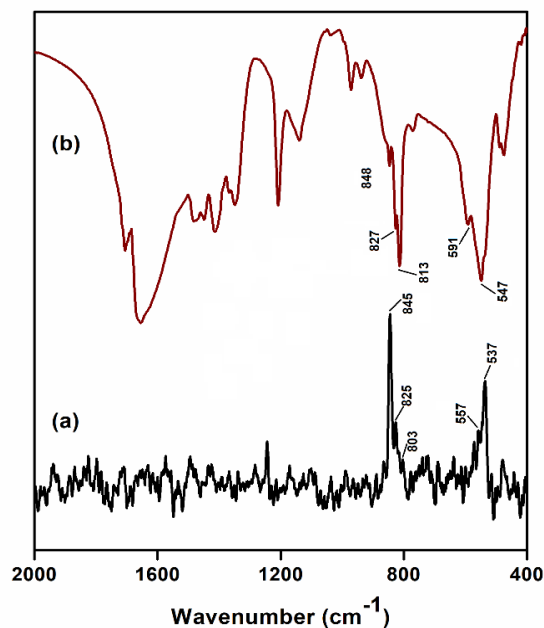


**Fig. 4.3** (a) Raman spectrum and (b) FTIR spectrum of **NbPMA (4.1)**.

compared to that of the free ligand suggested the unidentate coordination of the carboxylate group in the macromolecular complex [44,51]. It is notable that analogous mode of coordination has been observed in case of **PMA** anchored V and Mo complexes reported previously by our group [44,46]. The peak observed at *ca.* 1703  $\text{cm}^{-1}$  in the spectrum of **NbPMA (4.1)** indicated the presence of free -COOH in the compound.

#### 4.3.2.3 Electronic spectral studies

The UV-Vis spectrum of the macromolecular complex **NbPMA (4.1)** depicted in **Fig. 4.4**, was recorded in an aqueous solution. The spectrum showed a weak absorbance at around 350 nm typically due to the peroxido-to-metal (LMCT) transition of triperoxido-Nb species (**Fig. 4.4**) [52,53].

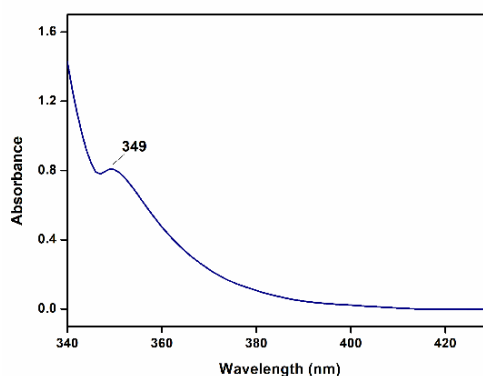


**Fig. 4.4** UV-Visible absorption spectrum of **NbPMA (4.1)**.

#### 4.3.2.4 $^{13}\text{C}$ NMR analysis

The  $^{13}\text{C}$  NMR spectra of the water-soluble compound **4.1** and the corresponding original polymer, **PMA** recorded in  $\text{D}_2\text{O}$  are presented in **Fig. 4.5**. The chemical shift data are listed in **Table 4.2**. The spectrum of the virgin polymer **PMA** displayed a carboxylate carbon signal at *ca.* 187 ppm (**Fig. 4.5, Table 4.2**), along with the other signals originating from the chain carbon atoms [54,55]. In the spectrum of pNb anchored complex, the presence of an additional peak at a much lower field of *ca.* 221 ppm assignable to coordinated  $\text{COO}^-$  group signified participation of the carboxylate group in complexation. The considerable downfield shift,  $\Delta\delta$  ( $\delta_{\text{complex}} - \delta_{\text{free carboxylate}}$ )  $\approx$  34 ppm suggested the presence of strong metal-ligand interaction in the macromolecular complex [44,51,52]. The observation is in conformity with some other polyacrylate and **PMA**-bound peroxidometal systems reported earlier [43,44,46,56,57].

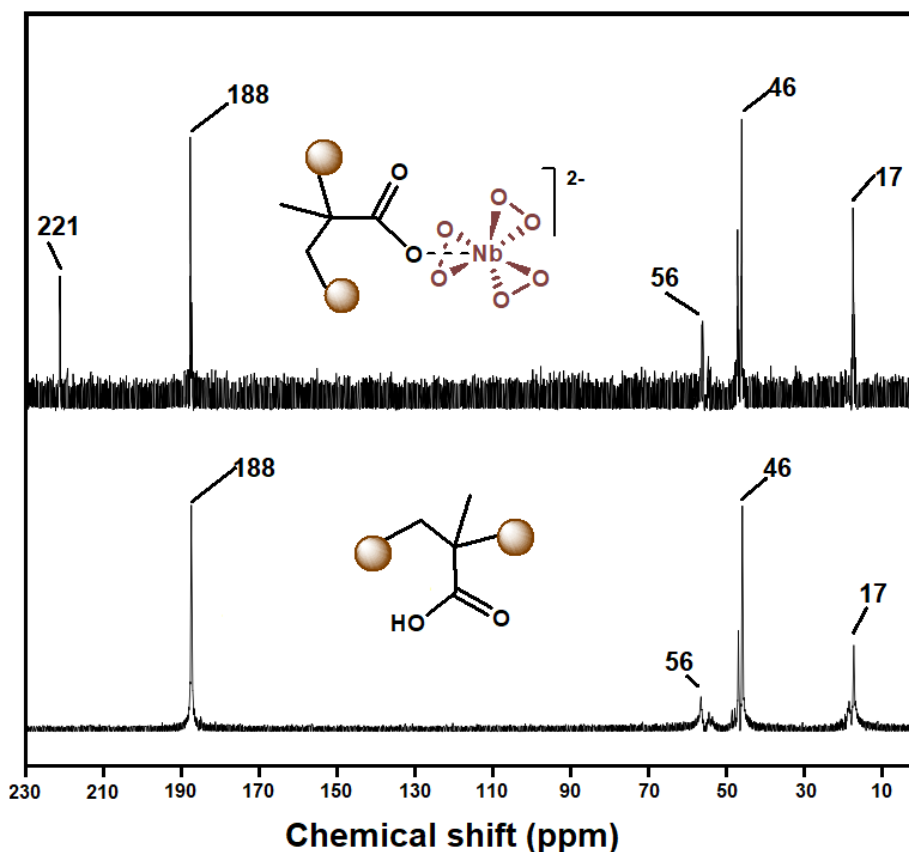


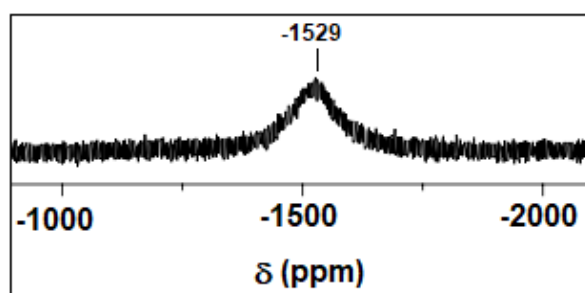
**Fig. 4.5**  $^{13}\text{C}$  NMR spectra of (a) **PMA** and (b) **NbPMA (4.1)** in  $\text{D}_2\text{O}$ .

**Table 4.2:**  $^{13}\text{C}$  NMR chemical shifts of the polymer-bound complex

Compound	Chemical Shift (ppm)				
	$\text{CH}_3$	Quaternary carbon	$\text{CH}_2$	Carboxylate	
				Free	Complexed
<b>PMA</b>	17.28	45.89	56.46	187.58	-
<b>NbPMA</b>	17.41	46.08	56.56	187.84	221.46

#### 4.3.2.5 $^{93}\text{Nb}$ NMR analysis

Crucial information can be derived regarding the local environment of Nb in a compound employing  $^{93}\text{Nb}$  NMR analysis, as  $^{93}\text{Nb}$  NMR resonance is sensitive to the coordination number of Nb sites [58]. The  $^{93}\text{Nb}$  NMR spectrum of compound **NbPMA (4.1)** in an aqueous solution displayed a single resonance at around -1529 ppm (**Fig. 4.6**) which is in the region characteristic of eight coordinated environment for Nb [58,59]. The presence of only one signal in the spectrum further showed the existence of Nb(V) in a single coordination environment in the compound. The position and pattern of the peak thus validate the formula assigned and resembled closely the spectra of other pNb complexes bound to polyacrylate and polystyrene sulphonate macromolecules reported previously by our group [42,56]. It is likely that inter-chain interaction between the **PMA** bound triperoxido-Nb(V) centers and neighbouring pendant carboxylate groups of the polymer chain would result in the completion of eightfold coordination around each Nb(V) center in **NbPMA (4.1)**, as has been observed in a majority of the reported pNb complexes [42, 47,49,52,56].

**Fig. 4.6**  $^{93}\text{Nb}$  NMR spectrum of **NbPMA (4.1)** in  $\text{D}_2\text{O}$ .

### 4.3.2.6 Thermogravimetric Analysis

Thermogram of the compound **NbPMA (4.1)** is shown in **Fig. 4.7** and the respective mass loss values are shown in **Table 4.3**. The compound **4.1** undergoes three-stage of degradation upon the increase of temperature up to 700 °C as depicted in **Fig. 4.7** and **Table 4.3**. The complex showed the first step of degradation occurring within the range of 48-97 °C corresponding to the liberation of lattice water from the complex. This step was followed by the loss of the coordinated peroxido groups from the complex in the range of 107-224 °C [42,56]. A broad degradation step observed within 312-594 °C is attributable to the decomposition of the base polymer [44,46]. The final residue left after complete degradation of the compound was identified as oxidoniobium species along with the char residue from the polymer as revealed by FTIR analysis.

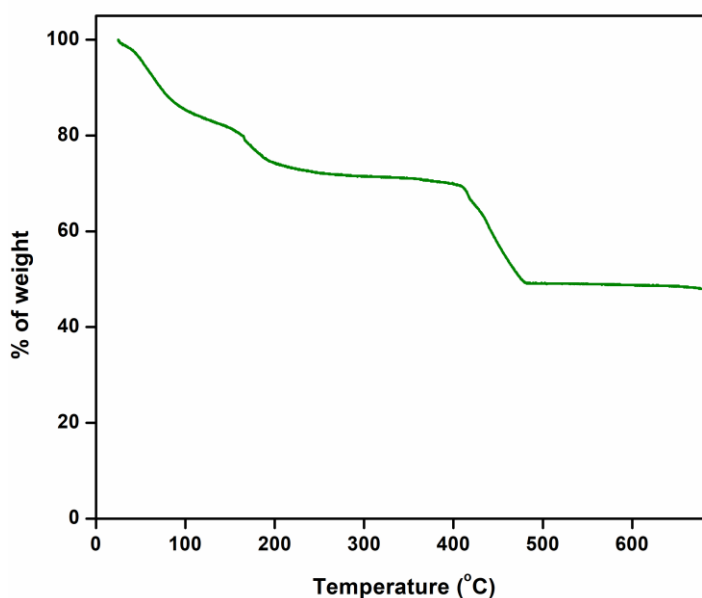


**Fig. 4.7** Thermogram of **NbPMA (4.1)**.

**Table 4.3:** TGA data of the complex **NbPMA (4.1)**

Compound	Temperature range (°C)	Observed weight loss (%)	Final residue (%)
<b>Nb-PMA</b>	48-97	10.7	55.0
	107-224	11.7	
	312-594	22.6	

---

### 4.3.3 Catalytic performances of the polymer-supported catalysts in the conversion of HMF to HMFCA

Having gained an access to two different types of immobilized peroxidoniobium systems, *viz.*, PS-DVB resin grafted peroxidoniobates **MRVNb (3.1)**, **MRNNb (3.2)** and **MRGNb (3.3)** (Chapter 3) and the water-soluble polymer anchored compound **NbPMA (4.1)**, we proceeded to investigate their efficacy as heterogeneous and homogeneous catalyst, respectively in HMF oxidation in an aqueous medium. In order to evaluate the appropriate reaction conditions to achieve the maximum HMF conversion and the desired product selectivity, the effects of main reaction parameters such as reaction temperature, catalyst loading, oxidant concentration, solvent, and the concentration of base were investigated. Optimization studies were conducted using **MRGNb (3.3)** as the representative catalyst.

First, a preliminary experiment was carried out in a basic aqueous solution maintaining Nb: HMF molar ratio of 1:50 and HMF: NaOH molar ratio of 1:2, using 2 equivalents of H<sub>2</sub>O<sub>2</sub>. The reaction was conducted at room temperature. The universal green solvent water was the solvent of choice in our study keeping in view the environmental aspect. Under these conditions, HMF was observed to undergo 24% conversion to selectively yield HMFCA as the sole reaction product after 90 min of reaction time. Significantly, no by-products such as FFCA, DFF, or FDCA were detected by HPLC under these reaction conditions.

#### 4.3.3.1 Effect of temperature

Subsequently, we have examined the performance of the catalyst at a moderately elevated temperature of 40 °C whilst keeping the other variables constant. As seen from the data reported in **Table 4.4** and **Fig. 4.8** a significant boost in HMF conversion occurred upon increasing the temperature from RT to 40 °C while HMFCA selectivity remained unaltered at 100%. Finally, we were pleased to find that quantitative transformation of HMF into the targeted product HMFCA with 100% selectivity could be attained at a temperature of 60 °C within 90 min of the stipulated reaction time. On increasing the temperature further to 80 °C, although the reaction proceeded with 100% HMF conversion, however, HMFCA selectivity was noted to decrease to nearly 74%, probably because of degradation of HMF occurring at a higher temperature. Thus, 60 °C emerged to be the optimized reaction temperature from our study. It is apparent that the

reaction temperature had a remarkable effect on the % conversion of HMF although the HMFCFA selectivity remained consistently high irrespective of the temperature employed. It is also obvious that no side product formation occurred under the applied conditions even at relatively higher temperature.

**Table 4.4:** Effect of temperature on HMF conversion to HMFCFA catalyzed by **3.3**<sup>a</sup>

Entry	Temperature	Conversion of HMF (%)	HMFCFA Selectivity (%)	TON <sup>b</sup>
1	RT	≥24	100	12
2	40°C	≥58	100	29
<b>3</b>	<b>60°C</b>	<b>100</b>	<b>100</b>	<b>50</b>
4	80°C	100	74	50

<sup>a</sup>Reaction conditions: HMF (0.4 mmol, 50.4 mg), 30% H<sub>2</sub>O<sub>2</sub> (0.8 mmol), catalyst (0.008 mmol of Nb), NaOH (0.8 mmol, 32 mg) in water (4 mL), 90 min. <sup>b</sup>TON (turnover number) = mmol of substrate consumed per mmol of Nb.

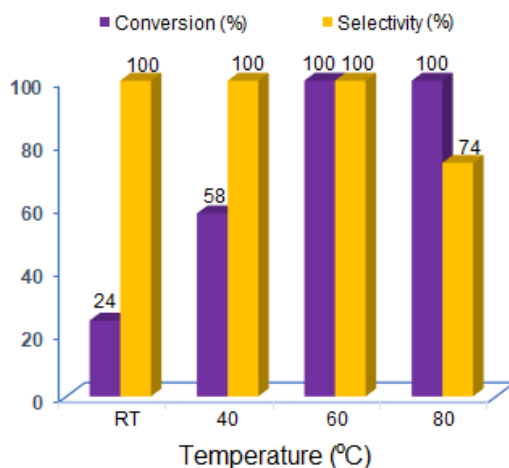


**Fig. 4.8** HMF conversion versus temperature (catalyst: **3.3**). Reaction conditions: as mentioned under **Table 4.4**.

#### 4.3.3.2 Effect of oxidant concentration

As the oxidant concentration is known to play a vital role in the successful selective oxidation of HMF, we have investigated the effect of H<sub>2</sub>O<sub>2</sub> concentration on HMF oxidation by using four different equivalents of 30% hydrogen peroxide ranging

between 0.5 to 2 equivalents. We have kept the concentrations of H<sub>2</sub>O<sub>2</sub> rather low, as it has been known that high H<sub>2</sub>O<sub>2</sub> concentration often triggers HMF degradation under the basic condition [35,36]. The results are summarized in **Table 4.5** and **Fig. 4.9**. It is remarkable that even with a 0.5 equivalent of H<sub>2</sub>O<sub>2</sub> a fairly good conversion of HMF occurred to selectively form HMFCFA. Further increase in H<sub>2</sub>O<sub>2</sub> concentration led to a gradual rise in HMF conversion till the quantitative conversion of HMF to HMFCFA was achieved with 2 equivalents of H<sub>2</sub>O<sub>2</sub>. Thus, HMF: H<sub>2</sub>O<sub>2</sub> molar ratio of 1:2 was found to be ideal to achieve maximum HMF conversion along with complete HMFCFA selectivity and a high TON value of 50, within a reasonably short reaction time.

**Table 4.5:** Effect of amount of H<sub>2</sub>O<sub>2</sub> on HMF oxidation to HMFCFA catalyzed by **3.3**<sup>a</sup>

Entry	Sub:H <sub>2</sub> O <sub>2</sub>	Conversion of HMF (%)	HMFCFA Selectivity (%)	TON
1	1:0.5	≥41	100	21
2	1:1	≥62	100	31
3	1:1.5	≥79	100	40
<b>4</b>	<b>1:2</b>	<b>100</b>	<b>100</b>	<b>50</b>

<sup>a</sup>Reaction conditions: HMF (0.4 mmol), catalyst **MRGNb (3.3)** (0.008 mmol of Nb, 29.6 mg), NaOH (0.8 mmol) in 4 mL water at 60 °C, 90 min.

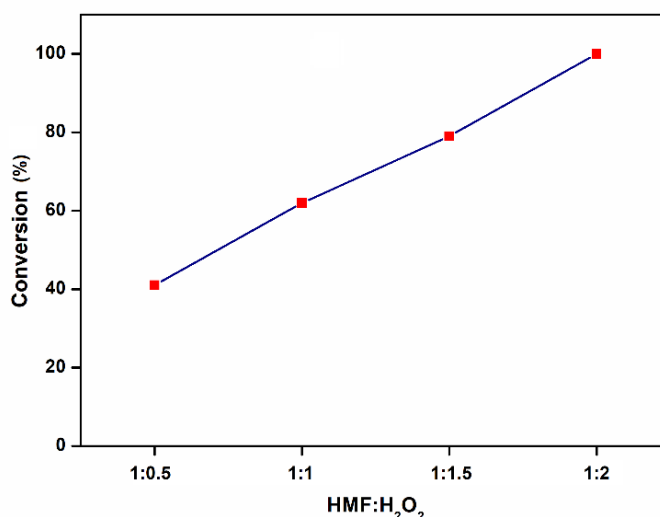


**Fig. 4.9** Effect of oxidant concentration in HMF conversion to HMFCFA. Reaction conditions: mentioned under **Table 4.5**.



### 4.3.3.3 Effect of catalyst amount

Our investigation on the influence of catalyst loading on HMF conversion and product selectivity revealed that, increasing the Nb: substrate molar ratio from 1:200 up to 1:50 resulted in a substantial improvement of % conversion. Complete HMF conversion could be achieved with Nb: substrate molar ratio of 1:50 (**Table 4.6** and **Fig. 4.10**). The reaction proceeded with 100% HMFCFA selectivity in each case. Thus, the molar ratio of 1:50 for Nb: substrate was found to be most favourable for the HMF oxidation reaction. The observed improvement in HMF conversion with the increment in catalyst loading is evidently a consequence of an increase in the availability of a number of catalytic active sites.

Most importantly, **MR** immobilized peroxidoniobium catalyst chemoselectively oxidized HMF into HMFCFA as an exclusive product irrespective of the amount of catalyst used and no additional side products were detected under the maintained experimental condition. Apparently, the catalyst is incapable of oxidizing the hydroxymethyl group of HMF in contrast to various other metal-catalyzed HMF oxidations which invariably led to further oxidation of HMFCFA into FFCA or FDCA [24,25,30,31].

**Table 4.6:** Effect of catalyst loading on HMF oxidation to HMFCFA catalyzed by **3.3**<sup>a</sup>

Entry	Cat:sub	Conversion of HMF (%)	HMFCFA Selectivity (%)	TON
1 <sup>b</sup>	-	≥20	83	-
2	1:200	≥44	100	88
3	1:150	≥51	100	77
4	1:100	≥68	100	69
<b>5</b>	<b>1:50</b>	<b>100</b>	<b>100</b>	<b>50</b>
6 <sup>c</sup>	1:50	≥42	100	21

<sup>a</sup>Reaction conditions: HMF (0.4 mmol), 30% H<sub>2</sub>O<sub>2</sub> (0.8 mmol), 60 °C, 90 min, NaOH (0.8 mmol) in water (4 mL) as solvent. <sup>b</sup>Blank reaction without any catalyst. <sup>c</sup>Using Na<sub>3</sub>[Nb(O<sub>2</sub>)<sub>4</sub>]·13H<sub>2</sub>O as catalyst (0.008 mmol of Nb).

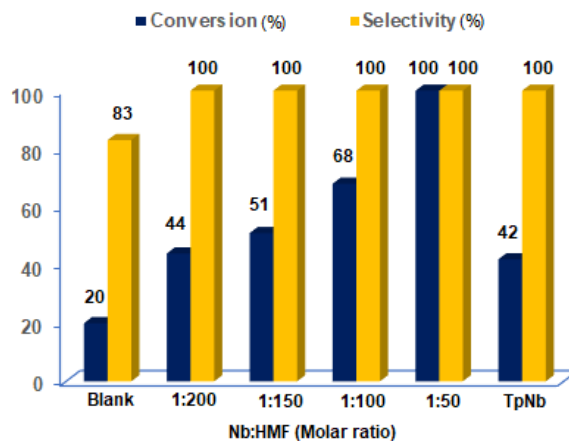


**Fig. 4.10** HMF conversion versus catalyst amount. Reaction conditions: mentioned under **Table 4.6**.

The blank reaction carried out excluding the catalyst under otherwise identical conditions provided 20% HMF oxidation with  $\text{H}_2\text{O}_2$ , within the stipulated reaction time [Table 4.6 (entry 1), Fig. 4.10]. The crucial role of the catalyst in accelerating the reaction is thus obvious from the low % conversion and HMFCa selectivity obtained in absence of the catalyst compared to the results attained using the polymer-supported catalyst. Moreover, when a reaction was conducted using the unsupported parent pNb complex  $\text{Na}_3[\text{Nb}(\text{O}_2)_4]$  instead of the polymer-supported catalyst maintaining the same Nb: HMF ratio [Table 4.6 (entry 6), Fig. 4.10], significantly lower conversion was observed. That the immobilization of the pNb species on polymer support has a significant impact on augmenting its catalytic efficiency is obvious from these findings.

#### 4.3.3.4 Effect of the amount of base

As evident from the available literature, base concentration is an important parameter that can significantly affect the oxidation as well as degradation of HMF [25,26,34,35]. The intermediate product of HMF oxidation, HMFCa has been reported to be stable in a basic environment [31]. However, high base concentrations can be detrimental to selectivity because of the formation of undesirable side reaction products [25,26,31]. The presence of an appropriate concentration of base in the reaction mixture is therefore necessary in order to control and minimize the formation of by-products from side reactions during HMF oxidation [25,26,31]. In the present study, we have used NaOH as a base to facilitate the reactions. The concentration of NaOH was optimized keeping the other reaction parameters constant for each experiment. The results shown in

**Table 4.7** (entry 1) and **Fig. 4.11** demonstrate that even in absence of base, the catalyst could facilitate HMF oxidation to selectively yield the desired HMFCFA although the HMF conversion was rather low. The addition of the base accelerated the reaction, establishing the important role played by the base in the selective and fast oxidation of HMF. It is notable that HMFCFA was identified as the exclusive reaction product under each of the applied conditions. From these data 2 equivalents of NaOH emerged to be the optimum and was used for subsequent experiments. At an HMF: base molar ratio of 1:3, HMFCFA selectivity dropped to 86% probably due to HMF degradation caused by relatively higher alkalinity.

**Table 4.7:** Impact of amount of base on the conversion of HMF to HMFCFA<sup>a</sup>

Entry	Sub:base	HMF Conversion (%)	HMFCFA Selectivity (%)	TON
1 <sup>b</sup>	-	≥15	100	8
2	1:1	≥66	100	33
<b>3</b>	<b>1:2</b>	<b>100</b>	<b>100</b>	<b>50</b>
4	1:3	100	86	50

<sup>a</sup>Reaction condition: HMF (0.4 mmol, 50.4 mg), 30% H<sub>2</sub>O<sub>2</sub> (0.8 mmol), catalyst (0.008 mmol of Nb) at 60 °C in water (4 mL) up to 90 min. <sup>b</sup>Reaction performed without base.

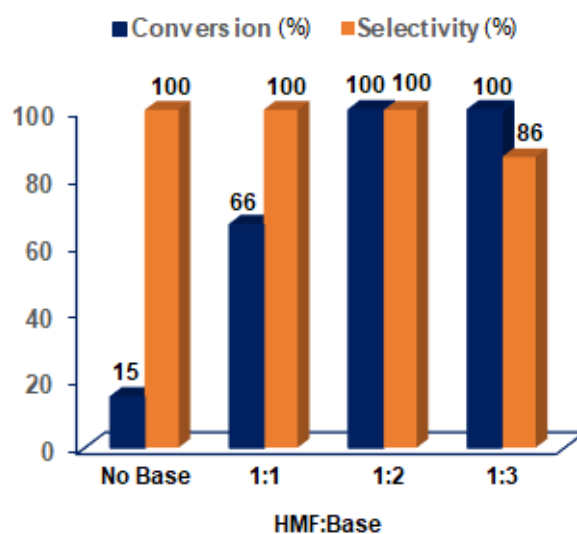


**Fig. 4.11** Impact of amount of base on the conversion of HMF to HMFCFA. Reaction conditions: mentioned under **Table 4.7**.

---

#### 4.3.3.5 Effect of reaction time

The % of HMF conversion with respect to time was studied over a span of 2 h and the result of time vs. HMF conversion profile is illustrated in **Table 4.8** and **Fig. 4.12**. Oxidation was observed to occur rapidly within the initial 15 min of starting the reaction to provide nearly 30% conversion of HMF. Notably, the reaction afforded the highest initial TOF of about  $64 \text{ h}^{-1}$  after just 15 min of reaction time. Subsequently, the reaction progressed with a steady increase in HMF conversion till *ca.* 90 min. Thus, the best results both in terms of 100% conversion as well as complete HMFCFA selectivity was obtained at a reaction time of 90 min (**Table 4.8**, **Fig. 4.12**). It is remarkable that, even on prolonging the reaction further to 2 h, HMFCFA was not further oxidized to other products. The observation once again demonstrates that the immobilized pNb catalyst is unable to oxidize the hydroxymethyl group under the applied conditions. Consequently, selective synthesis of HMFCFA was possible in the presence of polymer immobilized pNb catalysts leaving the alcohol group unaffected.

#### 4.3.3.6 Effect of solvent

We have screened the solvent effect on the activity of the catalyst by employing relatively safer halogen-free organic solvents, *viz.*, methanol, acetonitrile, and ethanol. As seen from the results listed in **Table 4.9** and **Fig. 4.13**, the reaction proceeded in each of the organic solvents with high product selectivity (**Fig. 4.13**) and moderate HMF conversion indicating the compatibility of the catalyst system with a wide range of solvents. Nevertheless, to our delight, the catalyst displayed superior activity with respect to both the conversion along with HMFCFA selectivity in an aqueous medium (**Table 4.9**, entry 1).

The findings are consistent with a number of previous reports demonstrating water to be the best solvent for HMF oxidation [26,31,34,35]. Davis *et al.* have also mechanistically established the importance of water in HMF oxidation from labelling experiments conducted with  $^{18}\text{O}_2$  and  $\text{H}_2^{18}\text{O}$  [14,60]. Furthermore, our observations are in accord with remarkable performances reported of Nb-based catalysts in aqueous phase organic reactions because of their high stability against hydrolysis and metal leaching [7,42,52,61,62].

**Table 4.8:** Effect of reaction time on HMF oxidation to HMFCFA by catalysts **MRGNb (3.3)** and **NbPMA (4.1)** with H<sub>2</sub>O<sub>2</sub><sup>a</sup>

Entry	Time (min)	<b>MRGNb (3.3)</b>				<b>NbPMA (4.1)</b>			
		Conversion of HMF (%)	HMFCFA Selectivity (%)	TON	TOF <sup>b</sup> (h <sup>-1</sup> )	Conversion of HMF (%)	HMFCFA Selectivity (%)	TON	TOF <sup>b</sup> (h <sup>-1</sup> )
1	15	≥30	100	16	64	≥39	100	20	78
2	30	≥49	100	25	50	≥69	100	35	70
3	45	≥72	100	36	48	≥84	100	42	56
4	60	≥88	100	44	44	≥93	100	47	47
5	75	≥95	100	48	38	<b>100</b>	<b>100</b>	<b>50</b>	<b>40</b>
6	<b>90</b>	<b>100</b>	<b>100</b>	<b>50</b>	<b>33</b>	100	100	50	33
7	120	100	100	50	25	100	100	50	25

<sup>a</sup>Reaction condition: HMF (0.4 mmol), 30% H<sub>2</sub>O<sub>2</sub> (0.8 mmol), catalyst (0.008 mmol of Nb), NaOH (0.8 mmol) 60 °C, water (4 mL). <sup>b</sup>TOF (turnover frequency) = mmol of substrate consumed per mmol of Nb per time.

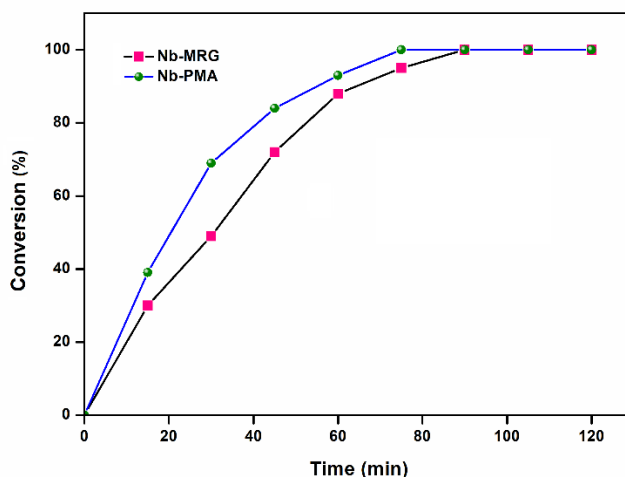


**Fig. 4.12** Effect of time on HMF oxidation by **3.3** and **4.1**. Reaction conditions: mentioned under **Table 4.8**.

**Table 4.9:** Effect of solvent on HMF oxidation to HMFCFA with H<sub>2</sub>O<sub>2</sub> catalyzed by **3.3**<sup>a</sup>

Entry	Solvent	HMF	HMFCFA	TON
		Conversion (%)	Selectivity (%)	
<b>1</b>	<b>H<sub>2</sub>O</b>	<b>100</b>	<b>100</b>	<b>50</b>
2	MeOH	≥57	100	29
3	EtOH	≥34	100	17
4	MeCN	≥48	100	24

<sup>a</sup>Reaction conditions: HMF (0.4 mmol), oxidant (0.8 mmol), catalyst (0.008 mmol of Nb), NaOH solution (0.8 mmol in 1 mL water), solvent (3 mL), 60 °C, 90 min.

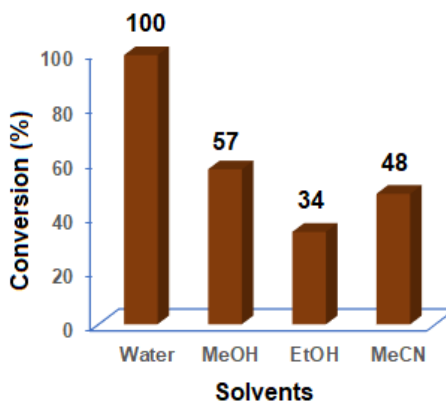


**Fig. 4.13** Effect of solvent on HMF conversion to HMFCFA. Reaction conditions: mentioned under **Table 4.9**.

Having standardized the optimum conditions for HMF oxidation with the heterogeneous catalyst **3.3**, we considered it worthwhile to explore the scope of the established catalytic protocol by examining the HMF oxidation over other two **MR**-supported pNb catalysts (**3.1** and **3.2**) and a Ta-based solid catalyst  $[\text{Ta}(\text{O}_2)_2(\text{Asn})_2]^-$ -**MR** (Asn = L-asparagine), reported previously from our laboratory [63]. It is worthy to mention that the Ta-based catalyst has previously been found to exhibit excellent activity in selective organic oxidations including olefin epoxidation and sulfide oxidation [63]. As anticipated, our results depicted in **Table 4.10** show that similar to the catalyst **3.3**, the other polymer anchored peroxido-metallate compounds also serve as highly efficient catalysts in  $\text{H}_2\text{O}_2$  induced oxidation of HMF into HMFCFA. From the relatively longer time required for the completion of HMF conversion in the case of Ta-based catalyst, it is clear that Nb-containing catalysts exhibit somewhat superior activity in comparison to the Ta-containing analog. (**Table 4.10**, entry 4).

**Table 4.10:** Oxidation of HMF over different polymer supported Nb and Ta catalysts<sup>a</sup>

Entry	Catalyst	Time (min)	% HMF Conversion	% HMFCFA Selectivity	TON	TOF <sup>b</sup> (h <sup>-1</sup> )
1	<b>MRVNb (3.1)</b>	90	100	100	50	64
2	<b>MRNNb (3.2)</b>	90	100	100	50	64
3	<b>MRGNb (3.3)</b>	90	100	100	49	62
4	$[\text{Ta}(\text{O}_2)_2(\text{Asn})_2]^-$ - <b>MR</b>	135	100	100	50	38
5	<b>NbPMA (4.1)</b>	75	100	100	50	78

<sup>a</sup>Reaction conditions: HMF (0.4 mmol), 30%  $\text{H}_2\text{O}_2$  (0.8 mmol), catalyst (0.008 mmol of Nb or Ta), 60 °C, NaOH (0.8 mmol), 4 mL water as solvent. <sup>b</sup>TOF (turnover frequency) = mmol of substrate consumed per mmol of Nb per time (determined from initial rates).

#### 4.3.3.7 HMF oxidation over homogeneous catalyst NbPMA (4.1)

Next, we examined the activity of the water-soluble compound **NbPMA (4.1)** as a homogeneous catalyst in HMF oxidation under the same optimized reaction conditions. Homogeneous catalysts are known to display relatively superior catalytic performance compared to their heterogeneous analog, although the recovery and recyclability of homogeneous systems are often considered tedious [64,65]. Interestingly, previous work

---

from our laboratory established that peroxido complexes of transition metals, *viz.*, Ti(IV), V(V), Nb(V), and Mo(VI) anchored to various water-soluble polymers could serve as highly efficient homogeneous catalysts in organic oxidations such as selective oxidation of sulfides to sulfoxide/sulfone and oxidative bromination in an aqueous medium, under mild reaction condition [42,43,46,66]. In this study, therefore, with the newly synthesized immobilized soluble peroxidoniobium compound **4.1** in hand, we considered it worthwhile to explore its catalytic potential in HMF oxidation *vis-à-vis* the heterogeneous counterparts **3.1-3.3**. As evident from the data shown in **Table 4.8** and **4.10** (entry 5), the catalyst **3.4** selectively provided 100% HMF conversion with complete product selectivity and the highest TOF value of  $78 \text{ h}^{-1}$ . The oxidation occurred within a shorter duration of reaction time of 75 min in comparison to the 90 min required for the heterogeneous catalysts **3.1-3.3**. The conversion versus time profiles of both types of catalysts presented in **Fig. 4.12** further showed that the homogeneous catalyst, **4.1** was noticeably more effective compared to the heterogeneous catalyst **3.3**.

#### 4.3.3.8 Recyclability of the catalysts

The stability and reusability of a catalyst system are of paramount importance for its practical utility. The recyclability of heterogeneous catalyst **MRGNb (3.3)** was examined up to 5 consecutive cycles of oxidation. The solid catalyst could be easily removed from the reaction system by centrifugation or simple filtration. After completion of the reaction, the recovered catalyst was washed with acetone, vacuum dried, and utilized in a fresh reaction run without further conditioning. **Fig. 4.14** reveals that the catalyst showed impressive recyclability up to five successive cycles without any alteration in the selectivity. In the case of the homogeneous catalyst **4.1**, the catalyst could not be recycled due to the difficulties encountered in separation from the organic products.

The recovered catalyst **MRGNb (3.3)** was subjected to FTIR and EDX spectral analyses to determine its stability. The FTIR spectrum (**Fig. 4.15**) of the reused catalyst displayed a close resemblance with that of the fresh catalyst. Furthermore, the EDX analysis indicated no quantitative loss in Nb content in comparison to the fresh complex.



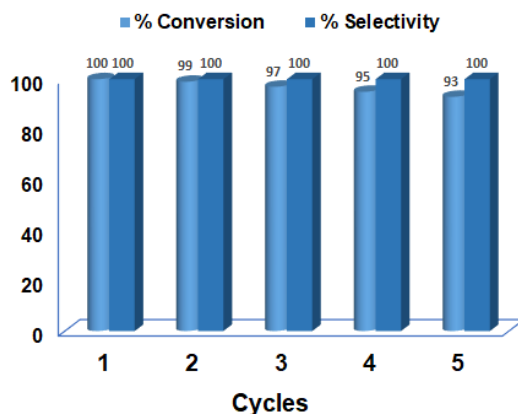


**Fig. 4.14** Reusability of **MRGNb (3.3)** for selective oxidation of HMF.

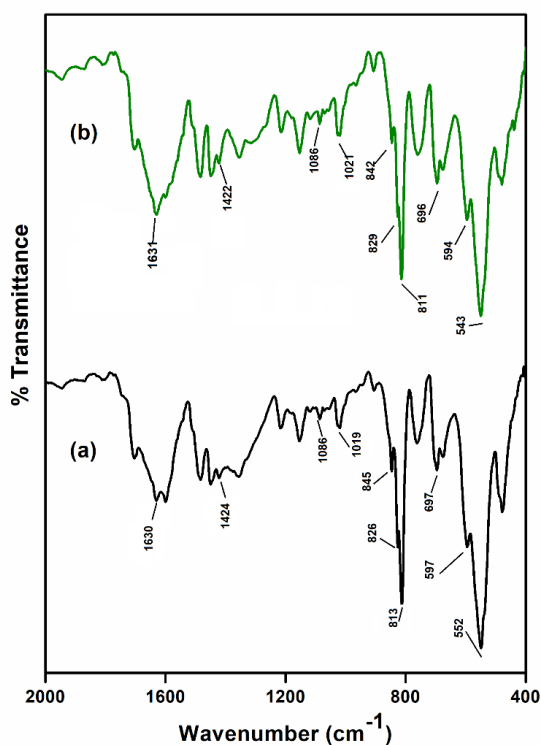


**Fig. 4.15** FTIR spectra of (a) **MRGNb** and (b) **MRGNb** after 5<sup>th</sup> cycle.

#### 4.3.3.9 Heterogeneity test

With an aim to verify the heterogeneity of the HMF oxidation process catalyzed by the solid catalyst **MRGNb (3.3)**, a standard hot filtration test was conducted under optimized condition and the results are shown in the **Fig. 4.16**. The solid catalyst was separated from the reaction mixture after 30 min of reaction (at about 50% of conversion) and the reaction was continued with the filtrate for further 1 h. The % conversion of the HMF did not increase significantly after the removal of the catalyst,

indicating the truly heterogeneous nature of the catalyst system. Moreover, AAS analysis of the filtrate showed no evidence of niobium in it, thereby ruling out the possibility of metal leaching from the polymer support.

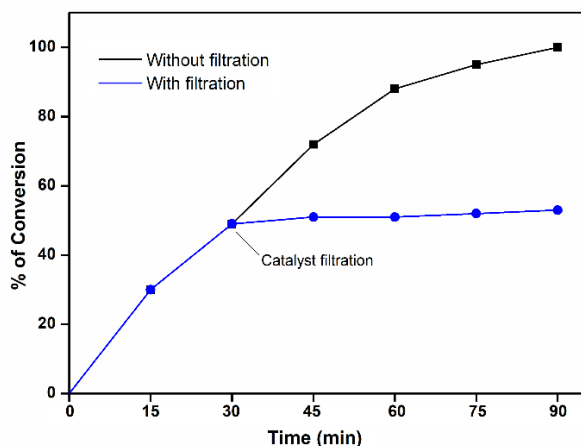


**Fig. 4.16** Hot filtration test for HMF oxidation to HMFCa by **MRGNb (3.3)**.

#### 4.4 Conclusions

To conclude, this chapter illustrates the extraordinary efficiency of simple polymer immobilized peroxidoniobium catalyst systems in the oxidation of HMF to afford selectively HMFCa with high TON and TOF values. The HMF oxidation was accomplished by employing aqueous  $\text{H}_2\text{O}_2$  as a liquid oxygen source, in a basic aqueous medium under mild condition. Importantly, no over-oxidation of HMFCa into by-products such as DFF, FFCA, and FDCA was observed to occur even on prolonging the reaction or increasing the temperature, indicating that the catalysts are incapable of oxidizing the hydroxymethyl group of HMF under the applied reaction conditions. This appears to be the first report on metal-catalyzed HMF oxidation where HMFCa could be quantitatively obtained with 100% selectivity. In addition to the high efficiency exhibited by both the catalyst systems, a significant strength of the heterogeneous catalyst compared to many other existing noble metal-based catalysts is its facile recyclability for multiple catalytic cycles with consistent activity/selectivity profile.

Apart from being an effective homogeneous oxidation catalyst, the water-soluble polymer anchored compound  $[\text{Nb}(\text{O}_2)_3(\text{carboxylate})]^{2-}$ -PMA (**NbPMA**, **4.1**) displayed distinct biochemical activity. The activity of **NbPMA (4.1)** as an inhibitor of phosphatase enzyme is described in Chapter 6.

---

**References**

1. Corma, A., Iborra, S., and Velty, A. Chemical routes for the transformation of biomass into chemicals. *Chemical Reviews*, 107(6):2411-2502, 2007.
2. Climent, M. J., Corma, A., and Iborra, S. Conversion of biomass platform molecules into fuel additives and liquid hydrocarbon fuels. *Green Chemistry*, 16(2):516-547, 2014.
3. Sheldon, R. A. Green and sustainable manufacture of chemicals from biomass: State of the art. *Green Chemistry*, 16(3):950-963, 2014.
4. Tirsoaga, A., El Fergani, M., Nuns, N., Simon, P., Granger, P., Parvulescu, V. I., and Coman, S. M. Multifunctional nanocomposites with non-precious metals and magnetic core for 5-HMF oxidation to FDCA. *Applied Catalysis B: Environmental*, 278:119309, 2020.
5. El Fergani, M., Candu, N., Tudorache, M., Granger, P., Parvulescu, V. I., and Coman, S. M. Optimized Nb-based zeolites as catalysts for the synthesis of succinic acid and FDCA. *Molecules*, 25(21):4885, 2020.
6. Mahendran, S., Srinivasan, V., Karthikeyan, G., and Pachamuthu, M. Selective oxidation of 5-hydroxymethylfurfural to 2, 5-diformylfuran over niobium incorporated MCM-41 catalyst. *Molecular Catalysis*, 510:111682, 2021.
7. Kang, S., Miao, R., Guo, J., and Fu, J. Sustainable production of fuels and chemicals from biomass over niobium based catalysts: A review. *Catalysis Today*, 374:61-76, 2021.
8. Rosatella, A. A., Simeonov, S. P., Frade, R. F., and Afonso, C. A. 5-Hydroxymethylfurfural (HMF) as a building block platform: Biological properties, synthesis and synthetic applications. *Green Chemistry*, 13(4):754-793, 2011.
9. Lewkowski, J. Synthesis, chemistry and applications of 5-hydroxymethylfurfural and its derivatives. *Arkivoc*, 1:17-54, 2001.
10. van Putten, R.-J., van der Waal, J. C., de Jong, E., Rasrendra, C. B., Heeres, H. J., and de Vries, J. G. Hydroxymethylfurfural, a versatile platform chemical made from renewable resources. *Chemical Reviews*, 113(3):1499-1597, 2013.
11. Sayed, M., Pyo, S.-H., Rehnberg, N., and Hatti-Kaul, R. Selective oxidation of 5-hydroxymethylfurfural to 5-hydroxymethyl-2-furancarboxylic acid using *Gluconobacter oxydans*. *ACS Sustainable Chemistry & Engineering*, 7(4):4406-4413, 2019.

- 
12. Zhang, X.-Y., Zong, M.-H., and Li, N. Whole-cell biocatalytic selective oxidation of 5-hydroxymethylfurfural to 5-hydroxymethyl-2-furancarboxylic acid. *Green Chemistry*, 19(19):4544-4551, 2017.
  13. Jia, H. Y., Zong, M. H., Yu, H. L., and Li, N. Dehydrogenase-catalyzed oxidation of furanics: Exploitation of hemoglobin catalytic promiscuity. *ChemSusChem*, 10(18):3524-3528, 2017.
  14. Davis, S. E., Benavidez, A. D., Gosselink, R. W., Bitter, J. H., de Jong, K. P., Datye, A. K., and Davis, R. J. Kinetics and mechanism of 5-hydroxymethylfurfural oxidation and their implications for catalyst development. *Journal of Molecular Catalysis A: Chemical*, 388:123-132, 2014.
  15. Pal, P. and Saravanamurugan, S. Recent advances in the development of 5-hydroxymethylfurfural oxidation with base (nonprecious)-metal-containing catalysts. *ChemSusChem*, 12(1):145-163, 2019.
  16. Gupta, K., Rai, R. K., and Singh, S. K. Metal catalysts for the efficient transformation of biomass-derived HMF and furfural to value added chemicals. *ChemCatChem*, 10(11):2326-2349, 2018.
  17. Zhou, H., Xu, H., Wang, X., and Liu, Y. Convergent production of 2, 5-furandicarboxylic acid from biomass and CO<sub>2</sub>. *Green Chemistry*, 21(11):2923-2927, 2019.
  18. Kucherov, F. A., Gordeev, E. G., Kashin, A. S., and Ananikov, V. P. Three-dimensional printing with biomass-derived PEF for carbon-neutral manufacturing. *Angewandte Chemie International Edition*, 56(50):15931-15935, 2017.
  19. Bello, S., Méndez-Trelles, P., Rodil, E., Feijoo, G., and Moreira, M. T. Towards improving the sustainability of bioplastics: Process modelling and life cycle assessment of two separation routes for 2, 5-furandicarboxylic acid. *Separation and Purification Technology*, 233:116056, 2020.
  20. Hirai, H. Oligomers from hydroxymethylfurancarboxylic acid. *Journal of Macromolecular Science: Part A - Chemistry*, 21(8-9):1165-1179, 1984.
  21. Munekata, M. and Tamura, G. Antitumor activity of 5-hydroxymethyl-2-furoic acid. *Agricultural and Biological Chemistry*, 45(9):2149-2150, 1981.
  22. Kucherov, F. A., Romashov, L. V., Galkin, K. I., and Ananikov, V. P. Chemical transformations of biomass-derived C6-furanic platform chemicals for sustainable

- 
- energy research, materials science, and synthetic building blocks. *ACS Sustainable Chemistry & Engineering*, 6(7):8064-8092, 2018.
23. Zhang, Z. and Deng, K. Recent advances in the catalytic synthesis of 2, 5-furandicarboxylic acid and its derivatives. *ACS Catalysis*, 5(11):6529-6544, 2015.
  24. Wang, F. and Zhang, Z. Cs-substituted tungstophosphate-supported ruthenium nanoparticles: An effective catalyst for the aerobic oxidation of 5-hydroxymethylfurfural into 5-hydroxymethyl-2-furancarboxylic acid. *Journal of the Taiwan Institute of Chemical Engineers*, 70:1-6, 2017.
  25. Schade, O. R., Kalz, K. F., Neukum, D., Kleist, W., and Grunwaldt, J. D. Supported gold- and silver-based catalysts for the selective aerobic oxidation of 5-(hydroxymethyl) furfural to 2, 5-furandicarboxylic acid and 5-hydroxymethyl-2-furancarboxylic acid. *Green Chemistry*, 20(15):3530-3541, 2018.
  26. An, J., Sun, G., and Xia, H. Aerobic oxidation of 5-hydroxymethylfurfural to high-yield 5-Hydroxymethyl-2-furancarboxylic acid by poly (vinylpyrrolidone)-capped Ag nanoparticle catalysts. *ACS Sustainable Chemistry & Engineering*, 7(7):6696-6706, 2019.
  27. Zhang, Z., Liu, B., Lv, K., Sun, J., and Deng, K. Aerobic oxidation of biomass derived 5-hydroxymethylfurfural into 5-hydroxymethyl-2-furancarboxylic acid catalyzed by a montmorillonite K-10 clay immobilized molybdenum acetylacetonate complex. *Green Chemistry*, 16(5):2762-2770, 2014.
  28. Kang, E. S., Kim, B., and Kim, Y. G. Efficient preparation of DHMF and HMFA from biomass-derived HMF via a Cannizzaro reaction in ionic liquids. *Journal of Industrial and Engineering Chemistry*, 18(1):174-177, 2012.
  29. Subbiah, S., Simeonov, S. P., Esperança, J. M., Rebelo, L. P. N., and Afonso, C. A. Direct transformation of 5-hydroxymethylfurfural to the building blocks 2, 5-dihydroxymethylfurfural (DHMF) and 5-hydroxymethyl furanoic acid (HMFA) via Cannizzaro reaction. *Green Chemistry*, 15(10):2849-2853, 2013.
  30. Donoeva, B., Masoud, N., and de Jongh, P. E. Carbon support surface effects in the gold-catalyzed oxidation of 5-hydroxymethylfurfural. *ACS Catalysis*, 7(7):4581-4591, 2017.
  31. Davis, S. E., Houk, L. R., Tamargo, E. C., Datye, A. K., and Davis, R. J. Oxidation of 5-hydroxymethylfurfural over supported Pt, Pd and Au catalysts. *Catalysis Today*, 160(1):55-60, 2011.
-

- 
32. Zhou, B., Song, J., Zhang, Z., Jiang, Z., Zhang, P., and Han, B. Highly selective photocatalytic oxidation of biomass-derived chemicals to carboxyl compounds over Au/TiO<sub>2</sub>. *Green Chemistry*, 19(4):1075-1081, 2017.
  33. Gao, D., Han, F., Waterhouse, G. I., Li, Y., and Zhang, L. Porous nitrogen-doped carbons supporting Fe-porphyrins for the highly efficient catalytic oxidation of HMF to HMFA. *Biomass Conversion and Biorefinery*, 1-13, 2022.
  34. Zhao, D., Rodriguez-Padron, D., Luque, R., and Len, C. Insights into the selective oxidation of 5-hydroxymethylfurfural to 5-hydroxymethyl-2-furancarboxylic acid using silver oxide. *ACS Sustainable Chemistry & Engineering*, 8(23):8486-8495, 2020.
  35. Su, T., Liu, Q., Lü, H., Alasmary, F. A., Zhao, D., and Len, C. Selective oxidation of 5-hydroxymethylfurfural to 5-hydroxymethyl-2-furancarboxylic acid using silver oxide supported on calcium carbonate. *Molecular Catalysis*, 502:111374, 2021.
  36. Chen, C. T., Nguyen, C. V., Wang, Z. Y., Bando, Y., Yamauchi, Y., Bazziz, M. T. S., Fatehmulla, A., Farooq, W. A., Yoshikawa, T., and Masuda, T. Hydrogen peroxide assisted selective oxidation of 5-hydroxymethylfurfural in water under mild conditions. *ChemCatChem*, 10(2):361-365, 2018.
  37. Li, S., Su, K., Li, Z., and Cheng, B. Selective oxidation of 5-hydroxymethylfurfural with H<sub>2</sub>O<sub>2</sub> catalyzed by a molybdenum complex. *Green Chemistry*, 18(7):2122-2128, 2016.
  38. Delidovich, I., Hausoul, P. J., Deng, L., Pfützenreuter, R., Rose, M., and Palkovits, R. Alternative monomers based on lignocellulose and their use for polymer production. *Chemical Reviews*, 116(3):1540-1599, 2016.
  39. Gao, L., Deng, K., Zheng, J., Liu, B., and Zhang, Z. Efficient oxidation of biomass derived 5-hydroxymethylfurfural into 2, 5-furandicarboxylic acid catalyzed by Merrifield resin supported cobalt porphyrin. *Chemical Engineering Journal*, 270:444-449, 2015.
  40. Saha, B., Gupta, D., Abu-Omar, M. M., Modak, A., and Bhaumik, A. Porphyrin-based porous organic polymer-supported iron(III) catalyst for efficient aerobic oxidation of 5-hydroxymethyl-furfural into 2, 5-furandicarboxylic acid. *Journal of Catalysis*, 299:316-320, 2013.

41. Passoni, L. C., Siddiqui, M. R. H., Steiner, A., and Kozhevnikov, I. V. Niobium peroxo compounds as catalysts for liquid-phase oxidation with hydrogen peroxide. *Journal of Molecular Catalysis A: Chemical*, 153(1-2):103-108, 2000.
42. Gogoi, S. R., Ahmed, K., Saikia, G., and Islam, N. S. Macromolecular metal complexes of Nb<sup>V</sup> as recoverable catalysts for selective and eco-compatible oxidation of organic sulfides in water. *Journal of Indian Chemical Society*, 95:801-812, 2018.
43. Ahmed, K., Saikia, G., Paul, S., Baruah, S. D., Talukdar, H., Sharma, M., and Islam, N. S. Water-soluble polymer anchored peroxotitanates as environmentally clean and recyclable catalysts for mild and selective oxidation of sulfides with H<sub>2</sub>O<sub>2</sub> in water. *Tetrahedron*, 75(44):130605, 2019.
44. Boruah, J. J., Kalita, D., Das, S. P., Paul, S., and Islam, N. S. Polymer-anchored peroxo compounds of vanadium(V) and molybdenum(VI): Synthesis, stability, and their activities with alkaline phosphatase and catalase. *Inorganic Chemistry*, 50(17):8046-8062, 2011.
45. Das, S. P., Ankireddy, S. R., Boruah, J. J., and Islam, N. S. Synthesis and characterization of peroxotungsten(VI) complexes bound to water soluble macromolecules and their interaction with acid and alkaline phosphatases. *RSC Advances*, 2(18):7248-7261, 2012.
46. Kalita, D., Sarmah, S., Das, S. P., Baishya, D., Patowary, A., Baruah, S., and Islam, N. S. Synthesis, characterization, reactivity and antibacterial activity of new peroxovanadium(V) complexes anchored to soluble polymers. *Reactive and Functional Polymer*, 68(4):876-890, 2008.
47. Bayot, D. and Devillers, M. Peroxo complexes of niobium(V) and tantalum(V). *Coordination Chemistry Reviews*, 250(19-20):2610-2626, 2006.
48. Djordjevic, C. and Vuletic, N. Coordination complexes of niobium and tantalum. V. Eight-coordinated di- and triperoxoniobates(V) and -tantalates(V) with some nitrogen and oxygen bidentate ligands. *Inorganic Chemistry*, 7(9):1864-1868, 1968.
49. Bayot, D., Devillers, M., and Peeters, D. Vibrational spectra of eight-coordinate niobium and tantalum complexes with peroxo ligands: A theoretical simulation. *European Journal of Inorganic Chemistry*, 4118-4123, 2005.
50. Nakamoto, K. *Infrared and Raman Spectra of Inorganic and Co-ordination Compounds, Part B*. Wiley and Sons, New York, 1997.

- 
51. Deacon, G. and Phillips, R. Relationships between the carbon-oxygen stretching frequencies of carboxylato complexes and the type of carboxylate coordination. *Coordination Chemistry Reviews*, 33(3):227-250, 1980.
  52. Gogoi, S. R., Boruah, J. J., Sengupta, G., Saikia, G., Ahmed, K., Bania, K. K., and Islam, N. S. Peroxonio niobium(V)-catalyzed selective oxidation of sulfides with hydrogen peroxide in water: A sustainable approach. *Catalysis Science & Technology*, 5(1):595-610, 2015.
  53. Maniatakou, A., Makedonas, C., Mitsopoulou, C. A., Raptopoulou, C., Rizopoulou, I., Terzis, A., and Karaliota, A. Synthesis, structural and DFT studies of a peroxoniobate complex of the biological ligand 2-quinaldic acid. *Polyhedron*, 27(16):3398-3408, 2008.
  54. Asada, M., Asada, N., Toyoda, A., Ando, I., and Kurosu, H. Side-chain structure of poly (methacrylic acid) and its zinc salts in the solid state as studied by high-resolution solid-state  $^{13}\text{C}$  NMR spectroscopy. *Journal of Molecular Structure*, 244:237-248, 1991.
  55. Díez-Peña, E., Quijada-Garrido, I., Barrales-Rienda, J. M., Wilhelm, M., and Spiess, H. W. NMR studies of the structure and dynamics of polymer gels based on N-isopropylacrylamide (NiPAAm) and methacrylic acid (MAA). *Macromolecular Chemistry and Physics*, 203(3):491-502, 2002.
  56. Saikia, G., Gogoi, S. R., Boruah, J. J., Ram, B. M., Begum, P., Ahmed, K., Sharma, M., Ramakrishna, G., Ramasarma, T., and Islam, N. S. Peroxo Compounds of vanadium(V) and niobium(V) as potent inhibitors of calcineurin activity towards RII-phosphopeptide. *ChemistrySelect*, 2(21):5838-5848, 2017.
  57. Saikia, G., Talukdar, H., Ahmed, K., Gour, N. K., and Islam, N. S. Tantalum(v) peroxido complexes as phosphatase inhibitors: A comparative study *vis-a-vis* peroxidovanadates. *New Journal of Chemistry*, 45(29):12848-12862, 2021.
  58. Lapina, O. B., Khabibulin, D. F., Romanenko, K. V., Gan, Z., Zuev, M. G., Krasil'nikov, V. N., and Fedorov, V. E.  $^{93}\text{Nb}$  NMR chemical shift scale for niobia systems. *Solid State Nuclear Magnetic Resonance*, 28(2-4):204-224, 2005.
  59. Papulovskiy, E., Shubin, A. A., Terskikh, V. V., Pickard, C. J., and Lapina, O. B. Theoretical and experimental insights into applicability of solid-state  $^{93}\text{Nb}$  NMR in catalysis. *Physical Chemistry Chemical Physics*, 15(14):5115-5131, 2013.



60. Davis, S. E., Zope, B. N., and Davis, R. J. On the mechanism of selective oxidation of 5-hydroxymethylfurfural to 2, 5-furandicarboxylic acid over supported Pt and Au catalysts. *Green Chemistry*, 14(1):143-147, 2012.
61. Ziolk, M. Niobium-containing catalysts—the state of the art. *Catalysis Today*, 78(1-4):47-64, 2003.
62. Selvaraj, M., Kawi, S., Park, D., and Ha, C. A merit synthesis of well-ordered two-dimensional mesoporous niobium silicate materials with enhanced hydrothermal stability and catalytic activity. *The Journal of Physical Chemistry C*, 113(18):7743-7749, 2009.
63. Saikia, G., Ahmed, K., Rajkhowa, C., Sharma, M., Talukdar, H., and Islam, N. S. Polymer immobilized tantalum(v)–amino acid complexes as selective and recyclable heterogeneous catalysts for oxidation of olefins and sulfides with aqueous H<sub>2</sub>O<sub>2</sub>. *New Journal of Chemistry*, 43(44):17251-17266, 2019.
64. Lindström, U. M. Stereoselective organic reactions in water. *Chemical Reviews*, 102(8):2751-2772, 2002.
65. Kitanosono, T., Masuda, K., Xu, P., and Kobayashi, S. Catalytic organic reactions in water toward sustainable society. *Chemical Reviews*, 118(2):679-746, 2018.
66. Boruah, J. J., Ahmed, K., Das, S., Gogoi, S. R., Saikia, G., Sharma, M., and Islam, N. S. Peroxomolybdate supported on water soluble polymers as efficient catalysts for green and selective sulfoxidation in aqueous medium. *Journal of Molecular Catalysis A: Chemical*, 425:21-30, 2016.